# Insights into the Effect of the PDMS-layer on the Kinetics and Thermodynamics of Analyte Sorption onto the Matrix-Compatible SPME Coating

Érica A. Souza-Silva†[1], Emanuela Gionfriddo[1], Md. Nazmul Alam[1], Janusz Pawliszyn[1]*.

† Current Address: Universidade Federal do Rio Grande do Sul, 91501-970 Porto Alegre, Rio Grande do Sul, Brazil

[1] Department of Chemistry, University of Waterloo, Waterloo, Ontario, Canada.

Corresponding author's name: Janusz Pawliszyn

Corresponding author's phone number: 1-519-888-4567 ext. 84641

Corresponding author's e-mail: janusz@sciborg.uwaterloo.ca

**ABSTRACT:** The currently presented research investigated the performance of matrix compatible PDMS-overcoated fibers (PDMS-DVB/PDMS) as compared to unmodified PDMS/DVB coatings using aqueous samples, and employing a wide range of analyte polarities, molecular weights, and functionalities. In the first part of the work, a kinetic approach was taken to investigate the effect of the PDMS outer layer on the uptake rate of analytes during the mass transfer process. In short, the results can be simplified into two models: (1) the rate-limiting step is the diffusion through the coating, and (2) the rate-limiting step is the diffusion through the aqueous diffusional boundary layer. For polar compounds, according to the theoretical discussion, the rate-limiting step is the diffusion through the coating; therefore, the outer PDMS layer influences the uptake rate into the matrix compatible coatings. On the other hand, for non-polar compounds, the rate-limiting step of the uptake process is diffusion through the aqueous diffusional boundary layer; as such, the overcoated PDMS does not affect uptake rate into the matrix-compatible coatings as compared to DVB/PDMS fibers. From a thermodynamic point of view, the calculated fiber constants further corroborate the hypothesis that the additional PDMS layer does not impair the extraction phase capacity.

When solid phase microextraction methods in direct immersion mode (DI-SPME) are to be employed towards analysis of complex matrices, it is important to ensure that matrix components do not impair the performance of the SPME device due to non-specific attachment of matrix components onto the coating surface. As presented in previous work[1], the implementation of a thin outer layer of PDMS onto the commercial PDMS/DVB coating has led to the achievement of a matrix-compatible coating surface. The developed configuration can be seen as a built-in membrane, utilizing a non-porous polymer, i.e. PDMS, placed between the sample and the DVB coating. This arrangement provides a protective layer surrounding the solid porous particles that constitute the coating and, moreover, allows for highly effective clean up and significant analyte enrichment.[1–3]

In fact, PDMS appears to be highly suitable for sampling in complex and challenging matrices; particularly, its employment can aid in the circumvention of problems resulting from surface-catalyzed analyte transformation and analyte competition for adsorptive sites, which can be occasionally observed for adsorbents.[4,5] Moreover, owing to the particular features of PDMS, such as its nontoxic nature, relative inertness, ease of fabrication, and well-known characterization, PDMS-based materials can be extensively used in a wide range of applications. [4,6–9]

Previous findings reported in the literature[1] investigated the PDMS-overcoated coating properties towards a single class of hydrophobic analytes, triazoles, where the PDMS outer layer did not substantially alter neither the kinetic nor the thermodynamic parameters associated with the original coating. The present work aimed at a more comprehensive investigation, extending the study towards an understanding of the effect of the PDMS outer layer on the extraction efficiency of the coating towards compounds with a wide range of polarities and diverse chemical functionalities.

One of the main premises behind the choice of PDMS as an overcoating polymer to create matrix-compatible coatings for food analysis is attributed to its hydrophobicity, which lessens the attachment of sugars and charged macromolecules to its surface. This process, in turn, significantly decreases the occurrence of fouling deriving from irreversible attachment of matrix components onto the coating surface during extraction or after thermal desorption. Moreover, the formation of artefacts due to reactions between carbohydrates and other matrix components at high temperatures is drastically minimized.[10]

Since PDMS materials are widely regarded as hydrophobic, the ability of any given compound to permeate through PDMS must be carefully investigated. Understanding the role of the PDMS outer layer in the PDMS-overcoated solid coating extraction process is particularly important when considering the following questions: (1) how does the PDMS outer layer affect the uptake of analytes for kinetic extractions (under non-equilibrium conditions)? (2) Would the PDMS layer impose a bias on the representativeness of sampling (polar vs non-polar analytes)? (3) Does the addition of the PDMS layer affect the coating capacity towards target analytes as compared to the original coating?

To address these questions, eleven analytes from various application classes (pesticides, industrial chemicals and pharmaceuticals) and with a wide range of log $K_{ow}$ values (ranging from 1.43 to 6) were selected to model and discuss the mass transfer of analytes within the PDMS-modified coating during the mass uptake process. In addition, the thermodynamic parameters of the coating, here associated with the fiber constants, were also investigated.

EXPERIMENTAL SECTION

Chemicals and Materials

All contaminant standards used in this study were Pestanal grade and kindly provided by Supelco (Bellefonte, PA, U.S.A.). PDMS/DVB Stableflex® fibers were purchased from Supelco. Sylgard 184® (PDMS pre-polymer and curing agent) was purchased from Dow Corning (Midland, MI, USA). Deionized water was obtained from a Barnstead/Thermodyne NANO-pure ultra-water system (Dubuque, IA, U.S.A.).

Standards and Samples Preparation

Individual solutions of standards were prepared in methanol at 1 or 2 mg/mL, with the exception of chlorothalonil, which was prepared in dichloromethane. A working standard mixture was prepared containing each contaminant in the range of 2.5 to 150 µg/mL. The concentration of each analyte was carefully chosen in order to guarantee enough analyte sensitivity for all tested coatings. A detailed list of chemical structures, log $K_{OW}$ values, concentrations, and the chemical structures for analytes in the working mixture is presented in Supplementary Information (Table S1 and Figure S1). To evaluate the amounts extracted for each analyte, a stock standard mixture with a concentration of 100 ng/µL was prepared in methanol. This stock solution was used for successive dilutions in order to obtain calibration solutions ranging from 0.5 to 80 ng/µL (8 levels). Liquid injections of calibration solutions were carried out in quadruplicates.

Preparation of the PDMS-modified coating

PDMS-modified coatings were prepared as described elsewhere,[1] with one noted exception: in the present procedure, the Sylgard 184® mixture was left to stand for 1h at room temperature before the coating procedure. This modification in procedure facilitated the attainment of a more viscous mixture owing to the initiation of the cross-linking process, which resulted in thinner and more homogenous coatings with only one immersion into the Sylgard 184 solution. PDMS-modified coatings were prepared by overcoating the commercially available PDMS/DVB fibers once (~ 10 µm PDMS layer) or twice (~ 30 µm PDMS layer).

All coatings were prepared at least in triplicate. Prior to their use, each coating was conditioned at 250 ℃ for one hour, and visually evaluated for uniformity and smooth surface coverage. If any defects were noted, coatings were discarded and new coatings prepared.

Instrumentation

Analyses were performed on an Agilent 6890 gas chromatograph (GC) and a 5973 quadrupole mass spectrometer (MS) (Agilent Technologies, CA, USA), coupled with a GERSTEL® cooled injection system (CIS) (GERSTEL GmbH, Mullheim, GE). Helium as the carrier gas was set to 1.5 mL/min. The injector was set at a temperature of 260 °C. Chromatographic separation was performed using a SLB®-5MS (30 m × 0.25 mm I.D, 0.25 µm) fused silica column (Sigma–Aldrich, Mississauga, ON, CA). The column temperature program was initially set at 40 °C for 2 min, ramped at 10°C/min to 180°C, then ramped at 20℃/min to 300℃ and held for 5 min, for a total run time of 25 min. The MSD transfer line temperature was set at 280∘C, while the MS Quad and MS source temperatures were set at 150∘C and 230∘C, respectively. The MS system was operated in electron ionization (EI) mode, and ion fragments were collected in the m/z 70–340 range. The quadrupole analyzer was operated in full scan mode: electron ionization (EI) at 70 eV, with a minimum of three ions chosen for identification of each analyte. Automated analysis was performed with a Gerstel multipurpose (MPS 2) autosampler (GERSTEL GmbH, Mullheim, GE) using the software Chemstation (Agilent Technologies, CA, USA), integrated with Maestro 1.3 (GERSTEL GmbH, Mullheim, GE). The MPS 2 autosampler was equipped with an Agitator-Stirrer that can either operate in agitation or stirring mode with the use of conventional magnetic stir bars.

SPME Procedure

The first employed approach was undertaken to compare the extraction kinetics between the commercial fiber PDMS/DVB and the PDMS-DVB/PDMS. An aliquot of 500 mL of nanopure water was spiked with 500 µL of working standard mixture and stirred for 5 min to ensure homogeneous distribution of analytes in the solution. Subsequently, an aliquot of 18 mL was transferred into a 20-mL vial containing a 0.5-inch teflon-coated stir bar. Concentrations of the individual compounds in the water sample ranged from 2.5 to 150 ng/mL. For the SPME procedure, a 1-min incubation of the sample at 35 ℃ was performed using the stirring feature of the MPS2 Gerstel autosampler instead of the conventionally employed agitation mode; in the agitation feature, the vial moves in relation to the fiber, causing a more turbulent flow, which would complicate the calculations presented further in this chapter. Automated extraction using stirring was set up so that the fiber pierced the vial cap septum 0.2 cm off-center. This arrangement ensured the establishment of a tangential flow direction of the sample to the fiber, thus enabling the use of semi-empirical relationships previously reported in the literature.[11] Extraction times ranged from 1 min to 120 min. Stirring velocities of 500 and 1500 rpm were investigated. Following extraction, fibers were placed in the GC injection port for desorption for 2 min at 270 ℃. All extraction time points were performed at least in duplicate.

The second approach aimed to compare thermodynamic parameters between the original PDMS/DVB fiber and the analogous PDMS-modified fibers. This was accomplished by investigating the capacities of these fibers. Fiber capacity was established by calculating the fiber constants ($f_c$), namely the product of the partitioning coefficient ($K_{fs}$) by the fiber volume ($V_f$). For this purpose, equilibrium extractions were performed at room temperature ($25 \pm 2$ °C) with 35 mL of water spiked with 20 µL of standard working mixture. Samples were placed in a 40-mL amber vial, with a special aluminum insert positioned between the hollow plastic cap and the septum to ensure accurate fiber positioning. Each sample was agitated using a teflon-coated stir bar (1 inch in length) with a magnetic stirrer (VWR 7x7'' ceramic hot plate/stirrer, 120V Pro). Following extraction, fibers were placed in the GC injection port for desorption for 2 min at 270 °C. All extraction time points were performed in duplicate.

RESULTS AND DISCUSSION

Kinetic Considerations

To investigate the rate-limiting step in the mass transfer of analytes through the aqueous diffusional boundary layer and the PDMS outer layer, extractions ranging from 1 to 120 min were performed for each coating. Subsequently, each profile was inspected within a range of short extraction times to identify the linear section of the mass uptake. Once the linear section of the mass uptake was established, the diffusion-based calibration model stated by Sukola et al. could be applied.[12]

As the thickness of the diffusional boundary layer is determined by both the agitation rate in the sample and by the diffusion coefficient of the analytes, within the same extraction process, the diffusional boundary layer will be different for different analytes. The employed experimental set-up (fiber exposed off-centre of the vial) provided a tangential flow direction of the sample with reference to the fiber, which allowed for the effective thickness of the diffusional boundary layer ($\delta_W$) to be estimated with the use of Equation 1[13], adapted from heat transfer theory:

$$\delta = 9.52 \left(\frac{b}{Re^{0.62} Sc^{0.38}}\right) \qquad \text{Equation 1}$$

Where $b$ is the radius of the fiber (135 µm for PDMS/DVB; 145 µm for 10 µm PDMS layer; and 165 µm for 30 µm PDMS layer), $Re$ is the Reynolds number ($Re = 2ub/v$; u is the linear velocity of the sample (10.6 cm/s for 500 rpm, and 31.9 cm/s for 1500 rpm) and $v$ is the kinematic viscosity of the matrix medium, here water), and $Sc$ is the Schmidt number ($Sc = v/D_W$; with $D_W$ as the diffusion coefficient of the analytes in the sample matrix; in this case, water). $D_W$ values ($cm^2/s$) calculated using the Hayduk and Laurie method[14] are presented in Supplementary Information Table S2.

To estimate the linear velocity, u, the following equation[13] was used:

$$u(r) = 1.05\pi Nr\left[2 - \left(\frac{r}{0.74R}\right)^2\right] \qquad \text{Equation 2}$$

Where $N$ is the magnetic stirrer speed in revolutions per second (8.33 for 500 rpm, and 25 for 1500 rpm), $r$ is the

distance between the fiber and the center of the vial (0.1965 cm), and $R$ is the radius of the stirring bar (0.635 cm).

The calculated diffusional boundary layer thicknesses are presented in Supplementary Information Table S3. As predicted by the mass transfer theory, an increase in agitation rate significantly decreased the thickness of the aqueous diffusional boundary layer, as the Reynolds number, used in Equation 2, decreased. In fact, a 3-fold increase in agitation rate led to an approximate 2-fold decrease in aqueous diffusional boundary layer thickness for all tested compounds. Conversely, since the additional PDMS layer was thinly applied in both the devices tested (10 and 30µm), the overall surface area does not change substantially, and only marginal differences were observed between fibers exposed to the same agitation rate. Regarding the analytes, as expected, larger analytes were noted to have thinner aqueous diffusional boundary layers than smaller molecules, such as nitrobenzene. This interplay exists owing to the lower diffusion coefficients of larger molecules in water (see Table S3), which causes them to take longer to cross the diffusional boundary layer and reach the coating surface.

Initial mass uptake rates were calculated for all cases by employing the least-square approximation method, using data obtained from extractions between 1 and 10 min. All determination coefficients ($R^2$) were > 0.99, showing good fit. Figure 1 presents two representative compounds for most polar analytes – namely, 1,3-dinitrobenzene (log $K_{ow}$ 1.43) and diazepam (log $K_{ow}$ 2.8). All other plots (nitrobenzene (log $K_{ow}$ 1.9); 2,6-dinitrotoluene (log $K_{ow}$ 2.42); chlorothalonil (log $K_{ow}$ 2.94); and 4-phenylphenol (log $K_{ow}$ 3.2)) can be found in Supporting Information Figure S2.
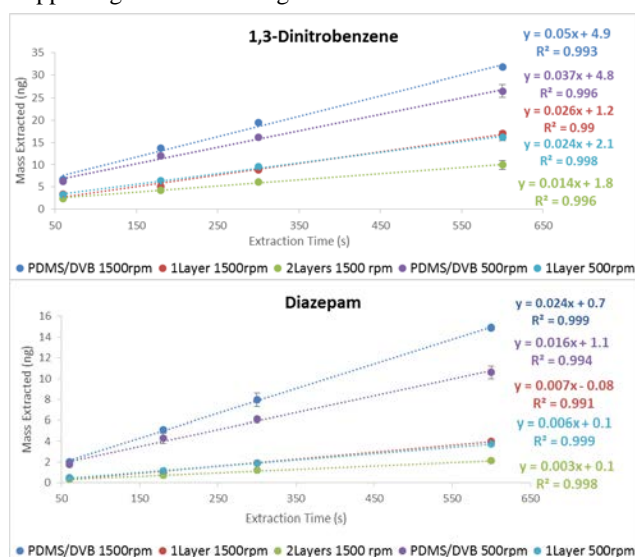


Figure 1: Mass uptake profiles of polar target analytes obtained from aqueous solutions at 30 °C.

For most polar compounds, the effect of the aqueous diffusional boundary layer, discerned by comparing the curves for PDMS/DVB acquired at sample agitation rates of 500 rpm (purple curve) and 1500 rpm (blue curve), was noted to

gradually increase as the size of the analytes (molecule volume) increased.

However, for both curves acquired using the fiber with the 10 µm PDMS layer (1 layer), mass transport through the PDMS barrier becomes the rate-limiting step (red curve for sample agitation rate of 1500 rpm, and light-blue curve for sample agitation rate of 500 rpm). In fact, a comparison of curves obtained at the same sample agitation rate of 1500 rpm with the 10 µm PDMS outer layer (1 layer) and with the 30 µm PDMS outer layer (2 layers) clearly evidences that the increase in PDMS layer thickness significantly hampers the mass uptake of these more polar analytes. For larger polar molecules, such as diazepam, given their low diffusivity in water ($D_w$ $5.87x10^{-6}$ cm$^2$/s), one would expect the effect of the aqueous diffusional boundary layer to play an important role in the resistance to mass uptake; however, this effect is concealed by the effect of the low $K_{PDMS,water}$, causing the outcome profiles to appear similar to smaller polar molecules. Therefore, for polar molecules, the thickness of PDMS ($^{TM}_{PDMS}$) will exert an accentuated effect on the uptake rates.

Additionally, the slower uptake rates of polar analytes extracted by PDMS-overcoated fibers could be attributed to the fumed silica fillers contained within the Sylgard 184 PDMS. These hydrophilic regions in the Sylgard 184 PDMS would allow for the immobilization of polar molecules via Langmuir-type adsorption. Such entrapment would slow down even further the permeation of these molecules, already characterized by low $K_{PDMS,water}$ values.[7]

As shown in Figure 2, for medium polarity analytes such as diazinon (log $K_{ow}$ 3.4) and parathion (log $K_{ow}$ 3.83), the effect of the aqueous diffusional boundary layer is seen when comparing both curves for PDMS/DVB (blue and purple curves), as well as in a comparison between both curves acquired using the fiber with the 10 µm PDMS outer layer (red and light-blue curves).

For parathion, contribution from the thickness of the aqueous diffusional boundary layer towards mass uptake was clearly diminished, as can be seen by comparing both curves obtained with the fiber coated with the 10 µm PDMS outer layer to both curves obtained with the PDMS/DVB fiber. As expected by their molecular volumes, the effect of the aqueous diffusional boundary layer thickness is more evident for diazinon ($D_w$ $5.75x10^{-6}$) than for parathion ($D_w$ $6.38x10^{-6}$). A closer inspection of the curves obtained at the same sample agitation rate of 1500 rpm with the 10 µm PDMS outer layer (1 layer) and the 30 µm PDMDS outer layer (2 layers) reveals the effect of PDMS layer thickness; the thicker the layer, the slower the mass uptake. For these analytes, exists a combination between the resistance imposed by the aqueous diffusional boundary layer and the PDMS layer, with the overall mass uptake being dependent on the magnitude of resistance imposed by these two barriers. Since both layers play a significant role in slowing down the mass uptake, it becomes somehow difficult to deconvolute the contribution of each layer in the mass transfer process in order to identify the rate-limiting step in the mass transfer process. For the most hydrophobic analytes, namely, trifluralin (log $K_{ow}$ 5.07), pendimethalin (log $K_{ow}$ 5.18), and p,p'-DDE (log $K_{ow}$ 6), the interpretation of the plots takes another direction, as presented in Figure 3. Examination of all curves obtained for trifluralin revealed the effect of the aqueous diffusional boundary layer as the rate-limiting step in all cases, which is expected given the low diffusivity of trifluralin in water. Interestingly, all curves pertaining to PDMS overcoated fibers exhibited faster uptake rates than PDMS/DVB. Given the high hydrophobicity of trifluralin, it can be understood that the accumulation of trifluralin on the sample/PDMS interface was facilitated by the PDMS layer (high $K_{PDMS,water}$); for the absorbent and hydrophobic PDMS extraction phase, the values of $K_{PDMS,water}$ correlate quite well with the hydrophobicity (i.e. $K_{ow}$) of the analytes. [15,16]
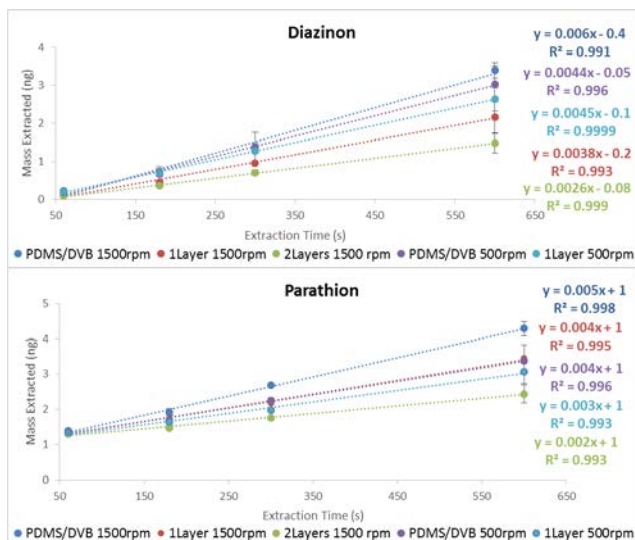


Figure 2: Mass uptake profiles of medium polarity target analytes obtained from aqueous solutions at 30 ºC.
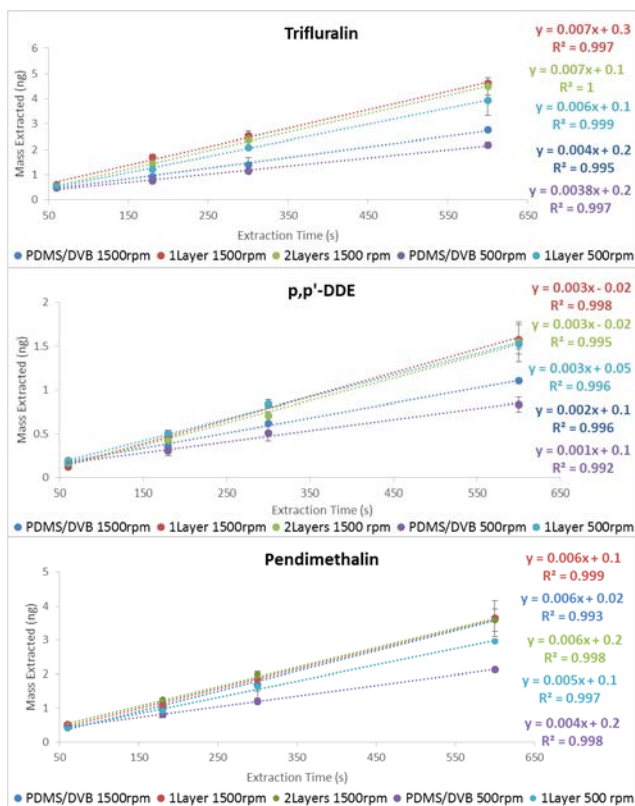
Figure 3: Mass uptake profiles of non-polar target analytes obtained from aqueous solutions at 30 °C.

For the most hydrophobic compound, p,p'-DDE, the boundary layer effect is clearly depicted when comparing both curves obtained with PDMS/DVB. Similarly to trifluralin, all curves obtained with the PDMS overcoated fibers have steeper curves regardless of sample agitation rate. The higher surface area of all PDMS-overcoated fibers, as compared to the non-modified PDMS/DVB, in conjunction with the very high value of $K_{PDMS,water}$ for p,p'-DDE, which may be a plausible explanation for the higher uptake rates obtained with PDMS-modified fibers. Indeed, it is well reported in the literature that amongst all commercially available SPME coatings, the PDMS coating has the highest affinity towards organochlorine pesticides, including p,p'-DDE. [17,18]

In the case of pendimethalin, the curves obtained at the same sample agitation rate of 1500 rpm for all fibers displayed the same uptake rate, which clearly evidences the aqueous diffusional boundary layer thickness as the rate-limiting step controlling the mass uptake of this large compound. It is important to note the differences in uptake rates when comparing the PDMS/DVB and 10 µm PDMS outer layers at lower sample velocities; the additional PDMS layer seems to favor the uptake of pendimethalin by the fiber, which could also be explained by the high $K_{PDMS,water}$ of pendimethalin.

A closer look into the parameters and functionalities of more hydrophobic molecules could shed some light into the sources of the differences observed in the uptake rates of pendimethalin as compared to those of trifluralin and p,p'-DDE. Frequently, a strong correlation is observed between

analyte size and transport properties in PDMS; generally, as analyte size increases, permeation in PDMS increases.[19] However, the difference between their molecular size is not very large, and based on the poor size selectivity of PDMS, it is quite unlikely that such differences stem from molecule size. A second possibility is associated with the plasticization effect, which is dependent on the magnitude of the $K_{PDMS,water}$ value for each analyte. Here, the rationale is that as the analyte concentration in the PDMS layer increases, a corresponding increase in PDMS local segmental motion can be observed, which in turn would increase analyte permeation in PDMS.[19] According to this approach, however, p,p-DDE would have enhanced permeation in the PDMS, given its larger log $K_{ow}$ value; hence, this hypothesis still does not explain the effect observed experimentally.

However, the diffusional boundary layer-controlled uptake observed for pendimethalin, and to a smaller degree for trifluralin, might be explained by taking into consideration the contribution of DVB towards the overall mass transfer process. Based on the structure of these analytes, high $K_{DVB,PDMS}$ values are expected due to the presence of nitrogenated groups, in addition to the benzene ring that offers great π-π interactions between molecules and the DVB sorbent. If the diffusion through the aqueous diffusional boundary layer is too slow to supply analytes to the PDMS layer, as compared to the rate of mass transfer from the PDMS layer to the DVB phase, a starvation effect takes place. As the starvation effect increases, the uptake rates become more aqueous- diffusional boundary layer controlled.[9] It is very important to note that based solely on the experiments performed and the data discussed, none of these hypotheses can be empirically confirmed at this point.

To better exemplify the PDMS-overcoated fiber system herein studied, the diagram shown in Figure 4 illustrates the expected mass transport process undertaken by analytes during extraction using a PDMS-overcoated fiber, where $^{TM}W$, $^{TM}PDMS$, and $^{TM}D$ are the thickness of the aqueous diffusional boundary layer, PDMS layer, and DVB sorbent, respectively; $C_0$ is the concentration of analyte in the bulk of the sample; $C_1$ is the concentration of analyte in the sample at the interface of PDMS and the sample diffusional boundary layer, $C_2$ is the concentration of analyte in the PDMS side at the interface of PDMS and the sample diffusional boundary layer; $C_3$ is the concentration of analyte in the PDMS side at the interface of PDMS and DVB sorbent; $C_4$ is the concentration of analyte at the DVB side at the interface of PDMS and DVB sorbent; and $C_5$ is the concentration of analyte at DVB inner-side at the fiber core interface.

In this discussion, the $K_{DVB,\ PDMS}$ is expected to be large for all compounds studied. Furthermore, the experimental design consisted of a low water concentration for all analytes (from 2.5 to 150 ng/mL) which makes it unlikely that localized displacement effects would occur. Based on the targeted analytes functionalities, the affinity of DVB towards said analytes is expected to be quite strong (high $K_{DVB,PDMS}$), owing to the presence of benzene rings as well as nitrogenated and oxygenated groups that offer great π-π interaction between analytes and DVB.

For a given sample velocity, smaller polar molecules (dashed black lines), such as 1,3-dinitrobenzene, are expected to rapidly diffuse through the aqueous diffusional boundary layer; since their diffusion coefficients are dependent on molecule size, this will result in higher $C_1$ values. However, due to the limited affinity of these polar molecules for PDMS (low $K_{PDMS,water}$), a lower $C_2$ value is then expected. Since DVB is expected to behave as a zero sink sorbent under the experimental conditions herein used, the concentration of analytes in the PDMS is expected to be zero at the PDMS/DVB interface, while a lower $C_2$ value, in turn, yields a smaller concentration gradient between $C_2$-$C_3$, thus resulting in decreased permeation for these compounds in the PDMS. The overall effect is that the PDMS layer becomes then the rate-limiting step in the mass uptake.
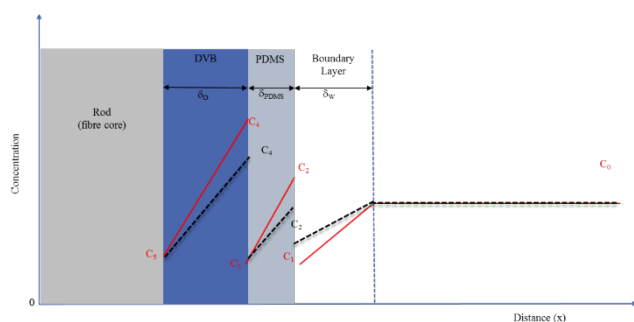


Figure 4- Process and concentration profile during analyte uptake using a PDMS-overcoated fiber (dashed black line – polar analytes; red line – non-polar analytes).

The trends marked in red in Figure 4 display the concentration profiles of larger and more hydrophobic compounds, such as p,p-DDE. The molecular size of p,p'-DDE leads to low diffusivity in water, while the aqueous diffusional boundary layer controls the uptake rate, resulting in a lower value of $C_1$. Conversely, these compounds are characterized by high $K_{PDMS,water}$ values, which enhance their permeation through the PDMS layer to an extent that the resistance imposed by the aqueous diffusional boundary layer thickness is concealed by their accumulation on the PDMS/sample interface ($C_2$). Moreover, given the very high $K_{PDMS,water}$ values, the PDMS acts also as a concentration medium.

As highlighted by the discussion above, $K_{PDMS,water}$ plays an important role in determining the effect of the PDMS outer layer on analyte uptake rate. In the PDMS-modified system, the movement of chemicals occurs through two contiguous layers, the aqueous diffusional boundary layer and PDMS layer, with each layer offering its own impedance on the mass transfer. The resistance imposed by the aqueous diffusional boundary layer to different analytes will be dependent on the diffusion coefficient of each analyte in water, which in turn depends on the size of a given molecule. In the PDMS layer, resistance is controlled by each analyte's permeation through the PDMS layer. The permeation of analytes through the PDMS layer is a product of the diffusion coefficient of a given analyte ($D_{PDMS}$) and its partitioning coefficient ($K_{PDMS,sample}$).

The permeation process occurs due to the difference between the concentrations of analytes in each side of the PDMS layer. In the system herein studied, the two sides are the interface sample/PDMS, and the interface PDMS/DVB. As previously stated, since DVB is a strong sorbent, and under the conditions used in this experiment can be said to behave as a "zero sink" for the target analytes, the concentration in the PDMS layer at the interface PDMS/DVB is kept at zero.

It is important to note that since PDMS has low diffusivity selectivity, the differences in permeation through the PDMS layer are mostly governed by their partition coefficients rather than the diffusivities in the polymer.[9,19] In fact, the diffusion coefficients of the targeted analytes in PDMS are smaller than the corresponding water coefficients by a factor of 5-6.[11] Accordingly, as $K_{PDMS,water}$ increases, the contribution of the rate-limiting barrier associated with the aqueous diffusional boundary layer is expected to become more pronounced.

Thermodynamic Considerations

PDMS is well known to be an absorbent media; in light of this, modification of solid SPME sorbents through application of an additional outer PDMS layer can potentially affect the overall coating capacity of the fiber. To address this point, thermodynamic parameters characterizing the coating, such as fiber constants, were investigated. For this purpose, 12h extractions were performed from aqueous samples, assuming the establishment of equilibrium conditions. The obtained results are presented in Table 1. As can be seen, similar amounts were extracted by both fibers (original PDMS/DVB and overcoated with 10 µm PDMS) for most analytes. A t-test paired two samples for means revealed that statistically different amounts ($p > 0.05$) were extracted only for 2,6-dinitrotoluene, trifluralin, and p,p'-DDE. In agreement with the results obtained in the previous subsection, an increase in the extracted amounts of trifluralin and p,p'-DDE was observed for the PDMS-overcoated fiber in comparison to PDMS/DVB, indicating that the PDMS layer also acts as a concentrating medium for analytes bearing high $K_{PDMS,water}$ values. Overall, the results obtained are in good agreement with the initial observations made for triazole analytes in our previous report.[1]

The fundamental thermodynamic principle of SPME involves the distribution of analytes between the sample medium and the extraction phase. The distribution constant defines the maximum enrichment factor achievable by a given extraction phase. For solid adsorptive coatings such as DVB, the active volume available for adsorption is not easily calculated, as it is dependent on the porosity displayed by the sorbent. In such cases, the coating capacity towards a given analyte can be measured by calculating the fiber constant, which is the product of the partitioning coefficient of an analyte between the sample and the solid coating ($K_{fs}$), and the volume of the coating ($V_f$). The fiber constant can be calculated as follows:

$$f_c = \frac{n_e V_s}{(C_0 V_s) - n_e}$$ Equation 3

Where $n_e$ is the amount of analyte extracted at equilibrium, $C_0$ is the analyte concentration in the sample, and $V_s$ is the sample volume. Using Equation 3, fiber constants were

calculated for all analytes extracted by both coatings; the obtained results are presented in Table 1.

The obtained $f_c$ data shows the insignificant effect of the PDMS overcoating on the equilibrium extraction of polar and mid-polar analytes when compared to the original PDMS/DVB coating. In fact, for polar and mid-polar analytes, fiber constants obtained with the PDMS-overcoated fiber were statistically similar to the ones obtained with the original PDMS/DVB coating, except for 2,6-dinitrotoluene. Conversely, for the most hydrophobic compounds, a noted increase was observed in the fiber constant for the PDMS-overcoated fiber, associated with the enhanced hydrophobic partitioning of these compounds into PDMS. In fact, the additional 10 µm of PDMS also acts as a concentrating medium for analytes bearing high $K_{PDMS,water}$ values, which adds to the overall coating capacity.

Table 1- Calculated fiber constants ($K_{fs}V_f$) for unmodified and PDMS-overcoated PDMS/DVB coatings.

| | | PDMS/DVB | | PDMS 10 µm Layer | |
|---|---|---|---|---|---|
| | log $K_{ow}$ | $f_c$ | C. V | $f_c$ | C. V. |
| 1,3-Dinitrobenzene | 1.43 | 0.39 | 0.05 | 0.29 | 0.05 |
| Nitrobenzene | 1.9 | 0.25 | 0.06 | 0.36 | 0.15 |
| 2,6-Dinitrotoluene | 2.42 | 1.174 | 0.004 | 0.89 | 0.14 |
| Diazepam | 2.8 | 0.51 | 0.07 | 0.51 | 0.05 |
| Chlorothalonil | 2.94 | 2.11 | 0.15 | 2.32 | 0.36 |
| 4-Phenylphenol | 3.2 | 2.68 | 0.32 | 2.71 | 0.22 |
| Diazinon | 3.4 | 8.32 | 0.17 | 8.60 | 0.67 |
| Parathion | 3.83 | 41.65 | 2.59 | 48.84 | 0.06 |
| Trifluralin* | 5.07 | 19.26 | 0.24 | 23.04 | 0.58 |
| Pendimethalin* | 5.18 | 50.27 | 1.57 | 56.65 | 0.04 |
| 4,4'-DDE* | 6 | 10.42 | 1.36 | 14.86 | 0.12 |

* Non-equilibrium conditions

### Computational Model

We have recently described a computational model that accounts for the analyte transport processes occurring during extraction by an SPME coating.[20,21] In the currently presented work, the previous model is extended through the inclusion of an extra domain (overcoating) around the fiber coating. As depicted in Figure S3, the model considers a two-dimensional segment of a sample-extractant system. The flow in the sample domain is governed by the Navier-Stokes equation, while the flow field is treated as steady. The time-dependent partial differential equations for each of these physical processes must be solved simultaneously. The procedure used to solve this problem is divided into two steps: (1) determination of the fluid velocity profile at a steady-state, assuming incompressible flow; and (2) use of this steady-state velocity profile as the initial condition to solve for the coupled transient mass transport and sorption equations. In the sample matrix, chemical transport is assumed to occur via convection and

diffusion, while diffusion is assumed as the only transport process occurring in the coating domain. Due to a concentration jump, mass fluxes are established across the interfaces. COMSOL Multiphysics 5.1, a finite element method (FEM) based software package, was utilized in this modeling and simulation study. The parameters used in the simulation are given in Table S4.

Finally, as exemplified for diazinon in Figure 5 below, the modelling confirmed the experimental data herein presented, and the combined information obtained in this study answers questions raised during the initial stages of development of a matrix-compatible coating first developed using triazole pesticides as model,[1] in the sense that it corroborates and validates the hypothesis that the extraction capabilities of the original coating towards a wide range of analyte sizes and polarities is not significantly affected by the addition of the PDMS outer layer. Additional modelling of process and concentration profile during analyte uptake using a PDMS-overcoated fiber can be found in Supplementary Information Figures S4 and S5.
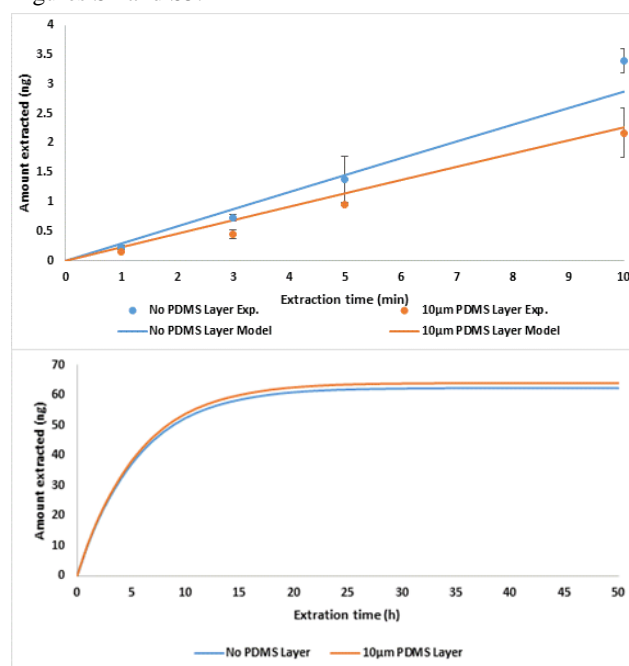


Figure 5 – Influence of PDMS outerlayer on diazinon extraction. (A) effect on analyte uptake during short extraction times. (B) effect on equilibration; here both equilibration time and the amount extracted for diazinon are not significantly influenced by the addition of 10 µm layer of PDMS.

### CONCLUSIONS

The currently presented research investigated the performance of PDMS-overcoated fibers versus that of the unmodified PDMS/DVB fiber using aqueous samples, employing a wide range of analyte polarities, molecular weights, and functionalities.

In the first part of the work, a kinetic approach was taken to investigate the effect of the PDMS outer layer on the rate of uptake of analytes during the mass transfer process. In short,

the results can be simplified in two models: (1) the rate-limiting step is the diffusion through the coating, and (2) the rate-limiting step is the diffusion through the aqueous diffusional boundary layer. For polar compounds, under the experimental conditions herein employed, and according to the theoretical discussion, the rate-limiting step is the diffusion through the overcoating; therefore, the overcoated PDMS layer affects the uptake rate. On the other hand, for non-polar compounds, the rate-limiting step is the diffusion through the aqueous diffusional boundary layer; therefore, the overcoated PDMS should not impair the uptake rate. While the PDMS-overcoated fibers have been proven to be robust and compatible for use in fruit pulp,[1] it is important to keep such kinetic considerations in mind throughout the development of methods aiming at simultaneous determinations of both polar and non-polar analytes, such as is the case in multiclass pesticide analysis. As previously stated, when employing adsorbent SPME coatings, short extractions are preferred as a means to extend the linearity range of the method, as well as to avoid inter-analyte displacement effects. However, if PDMS-overcoated fibers are to be employed, methods using too-short extraction times might not provide enough sensitivity towards most polar analytes.

The second part of this work aimed at investigating the thermodynamic parameters of the coating in view of potential changes in coating capacity resulting from application of the outer PDMS layer to the extraction phase. From a thermodynamic point of view, the calculated fiber constants further corroborate the hypothesis that the additional PDMS layer does not substantially change the extraction phase capacity. A positive effect, though, was observed for most hydrophobic analytes, where the additional PDMS layer also acted as a concentrating phase, increasing the coating capacity towards more hydrophobic analytes.

## ASSOCIATED CONTENT

### Supporting Information

Additional information as noted in text, namely: structures of model analytes employed in this study; representative chromatograms; diffusion coefficients in water; calculated boundary layer thicknesses; additional mass uptake profiles, as well as parameters for simulations and profiles obtained by Comsol modelling. This material is available free of charge via the Internet at http://pubs.acs.org.

## AUTHOR INFORMATION

### Corresponding Author

* janusz@sciborg.uwaterloo.ca

### Present Addresses

†Current Address: Universidade Federal do Rio Grande do Sul, 91501-970 Porto Alegre, Rio Grande do Sul, Brazil

### Author Contributions

The manuscript was written through contributions of all authors. All authors have given approval to the final version of the manuscript.

### Notes

The authors declare no competing financial interest.

## ACKNOWLEDGMENT

## REFERENCES

(1)     Souza-Silva, É. A.; Pawliszyn, J. *Anal. Chem.* **2012**, *84*, 6933–6938.
(2)     Souza-Silva, É. A.; Lopez-Avila, V.; Pawliszyn, J. *J. Chromatogr. A* **2013**, *1313*, 139–146.
(3)     Souza-Silva, É. A.; Gionfriddo, E.; Shirey, R.; Sidisky, L.; Pawliszyn, J. *Anal. Chim. Acta* **2016**.
(4)     Jahnke, A.; Mayer, P. *J. Chromatogr. A* **2010**, *1217*, 4765–4770.
(5)     Gionfriddo, E.; Souza-Silva, E. A.; Pawliszyn, J. *Anal. Chem.* **2015**.
(6)     Sia, S. K.; Whitesides, G. M. *Electrophoresis* **2003**, *24*, 3563–3576.
(7)     Harley, S. J.; Glascoe, E. A.; Maxwell, R. S. *J. Phys. Chem. B* **2012**, *116*, 14183–14190.
(8)     Johnston, I. D.; McCluskey, D. K.; Tan, C. K. L.; Tracey, M. C. *J. Micromechanics Microengineering* **2014**, *24*, 35017.
(9)     Seethapathy, S.; Górecki, T. *Anal. Chim. Acta* **2012**, *750*, 48–62.
(10)    Risticevic, S.; Souza-Silva, E. A.; DeEll, J. R.; Cochran, J.; Pawliszyn, J. *Anal. Chem.* **2015**, *88*, 1266–1274.
(11)    Pawliszyn, J. *Handbook of Solid Phase Microextraction*; Pawliszyn, J., Ed.; 1st ed.; Chemical Industry Press: Beijing, 2009.
(12)    Sukola, K.; Koziel, J.; Augusto, F.; Pawliszyn, J. *Anal. Chem.* **2001**, *73*, 13–18.
(13)    Pawliszyn, J. In *Solid Phase Microextraction: Theory and Practice*; Wiley-VCH: Waterloo, Ontario, Canada, 1997; pp. 43–96.
(14)    EPA. EPA On-line Tools for Site Assessment Calculation http://www.epa.gov/athens/learn2model/part-two/onsite/estdiffusion.html.
(15)    Shurmer, B.; Pawliszyn, J. *Anal. Chem.* **2000**, *72*, 3660–3664.
(16)    Paschke, A.; Popp, P. *J. Chromatogr. A* **2003**, *999*, 35–42.
(17)    López, R.; Goñi, F.; Etxandia, A.; Millán, E. *J. Chromatogr. B. Analyt. Technol. Biomed. Life Sci.* **2007**, *846*, 298–305.
(18)    Flores-Ramírez, R.; Ortiz-Pérez, M. D.; Batres-Esquivel, L.; Castillo, C. G.; Ilizaliturri-Hernández, C. A.; Díaz-Barriga, F. *Talanta* **2014**, *123*, 169–178.
(19)    Merkel, T. C.; Bondar, V. I.; Nagai, K.; Freeman, B. D.; Pinnau, I. *J. Polym. Sci. Part B Polym. Phys.* **2000**, *38*, 415–434.
(20)    Alam, M. N.; Pawliszyn, J. *Anal. Chem.* **2016**, *88*, 8632–8639.
(21)    Alam, M. N.; Ricardez-Sandoval, L.; Pawliszyn, J. *Anal. Chem.* **2015**, *87*, 9846–9854.

For TOC only